# Very high-current-density Nb/AlN/Nb tunnel junctions for low-noise submillimeter mixers

Jonathan Kawamura,[a] David Miller, Jian Chen,[b] and Jonas Zmuidzinas
*California Institute of Technology, 320-47, Pasadena, California 91125*

Bruce Bumble, Henry G. LeDuc, and Jeff A. Stern
*Center for Space Microelectronics Technology, Jet Propulsion Laboratory, Pasadena, California 91108*

We have fabricated and tested submillimeter-wave superconductor–insulator–superconductor (SIS) mixers using very high-current-density Nb/AlN/Nb tunnel junctions ($J_c \approx 30 \, \text{kA cm}^{-2}$). The junctions have low-resistance-area products ($R_N A \approx 5.6 \, \Omega \, \mu\text{m}^2$), good subgap-to-normal resistance ratios $R_{sg}/R_N \approx 10$, and good run-to-run reproducibility. From Fourier transform spectrometer measurements, we infer that $\omega R_N C = 1$ at 270 GHz. This is a factor of 2.5 improvement over what is generally available with Nb/AlOx/Nb junctions suitable for low-noise mixers. The AlN-barrier junctions are indeed capable of low-noise operation: we measure an uncorrected double-sideband receiver noise temperature of $T_{RX} = 110 \, \text{K}$ at 533 GHz for an unoptimized device. In addition to providing wider bandwidth operation at lower frequencies, the AlN-barrier junctions will considerably improve the performance of THz SIS mixers by reducing rf loss in the tuning circuits. © *2000 American Institute of Physics.* [S0003-6951(00)04915-9]

Niobium-based superconductor–superconductor (SIS) tunnel junction mixers have now achieved near-quantum-limited noise performance in the near-millimeter bands,[1] as was predicted to be possible theoretically.[2,3] This success relies heavily on advances in the technology for fabricating high-quality small-area niobium junctions with aluminum oxide barriers (Nb/AlOx/Nb), along with integrated Nb thin-film superconducting tuning circuits. The tuning circuits are necessary to overcome the frequency response limitation imposed by the finite resistance–capacitance ($R_N C$) product of SIS junctions: the 3 dB roll off in the frequency response ($\omega R_N C = 1$) of an untuned Nb/AlOx/Nb junction occurs at approximately 100 GHz. Here, $R_N$ is the junction normal resistance and $C$ is its capacitance.

An inductive tuning circuit with inductance $L$ allows the center frequency $\nu_0 = \omega_0/2\pi$ of the response to be chosen arbitrarily, according to the usual condition $\omega_0^2 L C = 1$, with a response bandwidth that is limited by the $R_N C$ product. Either a series or parallel inductance can be used, and is most often provided by a section of superconducting microstrip transmission line. In practice, rf losses in the tuning circuit seriously limit the performance at higher frequencies. Tuning circuits made from Nb become ineffective above 700 GHz, due to the onset of large Ohmic losses (surface resistance) above the superconducting energy-gap frequency $\nu_{gap} = 2\Delta/h$. At present, one of the main goals of SIS mixer development, driven by the needs of airborne and space-based astronomy projects, is to extend their low-noise performance to frequencies above 1 THz.

For operation above 700 GHz, a high conductivity normal metal (e.g., Al) can be used in place of niobium for the tuning circuit.[4] Another possibility is to use a low-loss su-

perconductor with a larger energy gap, such as NbTiN.[5] In either approach, the resulting resonant circuit requires a large quality factor ($Q \sim 10$ at 1 THz) for ideal performance and is, therefore, quite sensitive to Ohmic loss. For instance, in mixers which use normal metal tuning circuits, much of the rf power is still dissipated in the tuning circuit, and only a small fraction ($\sim 20\%$) of the signal is absorbed (detected) by the tunnel junction. High-frequency Ohmic loss is an important issue even for superconducting films (e.g., NbTiN), since the loss is often a sensitive function of film quality, composition, and microstructure, and can be difficult to control. In many SIS mixer designs, superconducting microstrip lines are also used for the impedance transformers which match the circuit to the rf feed, which can either be a planar antenna structure or a waveguide-to-microstrip transition. Although there may be losses in these transformers as well, the mixer's overall performance depends most critically on the inductive circuit which tunes out the junction capacitance, due to its high-$Q$ requirement.

Thus, an important parallel strategy is to reduce the junction $R_N C$ product, so that the $Q$ required for the tuning circuit is reduced and the mixer performance is less sensitive to losses. The $R_N C$ product is independent of junction area, but depends critically on the thickness of the tunnel barrier. Because the tunneling resistance decreases exponentially as the barrier thickness $t$ is reduced, while the capacitance should increase only as $1/t$, thinner tunnel barriers are needed to reduce the $R_N C$ product. Two parameters are commonly used to characterize the tunnel barrier: the Josephson critical current density $J_c$ and the resistance-area product $R_N A$. However, there is a serious practical difficulty associated with increasing the current density (reducing $R_N A$): at some point, the junction quality degrades rapidly.

An important figure of merit for SIS junctions used in low-noise mixer applications is the subgap-to-normal resistance ratio $R_{sg}/R_N$, which is a measure of the junction leak-

[a] Electronic mail: jhk@caltech.edu
[b] On leave from the Research Institute of Electrical Communication, Tohuku University, Sendai 980-8577, Japan.

age current. This quantity controls the conversion efficiency and noise of the mixer.[3] For Nb/AlOx/Nb junctions, the subgap-to-normal resistance ratio degrades rapidly for current densities much higher than 10 kA cm$^{-2}$.[6] This corresponds to a resistance-area product of $R_N A \approx 20 \, \Omega \, \mu m^2$. There is good evidence[7] that the quality degradation of Nb/AlOx/Nb tunnel junctions is caused by pinhole defects in the barrier. For $R_N A \approx 20 \, \Omega \, \mu m^2$, the junction specific capacitance is $C_s \approx 85 \, fF \, \mu m^{-2}$; combining these quantities, one obtains the roll-off frequency $(2 \pi R_N C)^{-1} \approx 100 \, GHz$ quoted above.

It is possible to fabricate high-quality junctions with higher current densities by using AlN as the barrier material.[8] We have recently fabricated Nb/AlN/Nb junctions with current densities as high as $J_c \approx 50 \, kA \, cm^{-2}$. The high-current-density AlN junctions have also been incorporated into submillimeter mixer circuits, using an existing design. This design, which was optimized for Nb/AlOx/Nb junctions with $J_c \approx 10 \, kA \, cm^{-1}$, has a well-understood behavior and has demonstrated excellent performance.[9] We assumed that this approach would be adequate, since the specific capacitance of AlN junctions was previously estimated to be roughly similar to that of AlOx junctions,[8] and since the capacitance should only be a slow function of current density.

The fabrication of the mixers largely followed the steps used to make the previous devices, with one exception. Instead of following the Al deposition by oxidation to form an oxide barrier, an AlN barrier was formed by plasma nitridation.[10] In this process, 7 nm of Al is sputtered on a Nb ground plane, and the nitride barrier is formed by exposing it to a pure nitrogen plasma. The ground plane and wiring layer Nb film are 170 and 300 nm thick, respectively. The junctions are square and have a nominal area in the range $A = 1.2 - 2.25 \, \mu m^2$. The target current density is $J_c \approx 30 \, kA \, cm^{-2}$, which yields junctions with $R_N A = 5.6 \, \Omega \, \mu m^2$. We obtain good subgap-to-normal resistance ratios, $R_{sg}/R_N \approx 10$. The current–voltage characteristics of one of the mixers are shown in Fig. 1. A batch of mixers with lower current density was also fabricated, with $R_N A = 20 \, \Omega \, \mu m^2$. These mixers have very similar $R_{sg}/R_N$ ratios as the high-current-density devices, which allow the mixer characteristics to be directly compared.

The mixer configuration we use is a quasioptical planar twin-slot antenna coupled to a two-junction tuning circuit.[11] The completed mixer chip is attached to an antireflection-coated hyperhemispherical Si lens. The lens and substrate are fitted into a copper mixer block assembly, which is mounted on a liquid-helium-cooled cold plate. The input beam passes through a high-density polyethylene lens at 4.2 K and several layers of infrared filtering provided by porous Teflon on the 77 K radiation shield. The vacuum window is a 25-$\mu$m-thick mylar film. The local oscillator is coupled to the input beam with a 12-$\mu$m-thick mylar beam splitter at room temperature. The intermediate frequency is centered at 1.5 GHz and the first-stage amplification is provided by a high-electron-mobility transistor amplifier with an input noise of $T_{if} \approx 5 \, K$.

The spectral response of 650 GHz mixers with both high and normal current densities was measured with Fourier
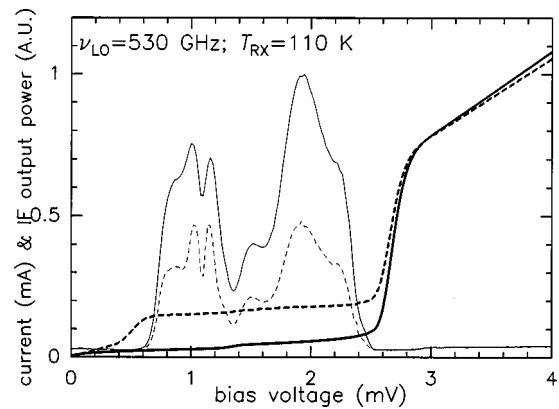


FIG. 1. Current–voltage ($I-V$) characteristics of a high-current-density 550 GHz mixer. The bath temperature is 4.2 K. Shown are the $I-V$ characteristics traced with (dashed heavy) and without (solid heavy) local-oscillator power applied. The LO frequency is 533 GHz, and the photon step begins at $V \approx 0.6 \, mV$. The if power in response to 295 K (solid light) and 77 K (dashed light) loads is shown as a function of voltage bias. The bumps in the if power response near $V \approx 1.2 \, mV$ reflect insufficient supression of Josephson currents. The mixer is normally biased near 2.0 mV for best performance. For this measurement, a 12.5 $\mu$m Mylar beam splitter was used to couple the optimum amount of LO power to the mixer, and $T_{RX} = 110 \, K$.

transform spectrometer (FTS), and the results are shown in Fig. 2. The difference between the two mixers is quite dramatic, as the response of the mixer with higher current density spans nearly an octave. FTS measurements were made on a number of other devices, and are summarized in Fig. 3. The response curves were fitted with a mixer model, which takes into account the frequency-dependent impedance of the slot antenna and the behavior of the tuning circuit. The surface impedance of the niobium films used in the microstrip transmission lines was calculated using Mattis–Bardeen theory in the local limit.[12] The model response was multiplied by the antenna main-beam efficiency to simulate the mixer's coupling to the FTS. In general, the main-beam efficiency varies only slowly near the center frequency but decreases rapidly at high frequencies due to the onset of large sidelobes in the antenna pattern.

The junction capacitance and normal-state resistivity of the niobium films are the main physical parameters that are derived by adjusting the mixer model to fit the measure-
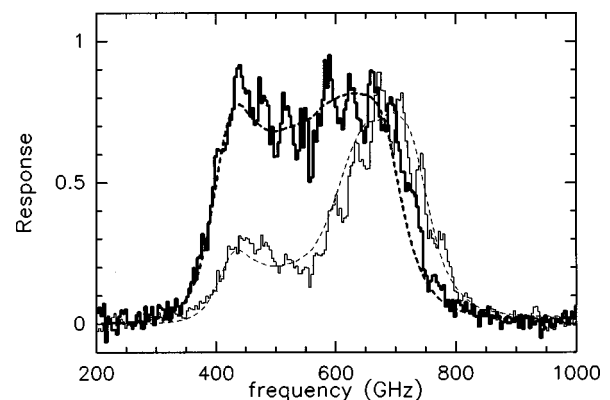


FIG. 2. Direct detection FTS response of Nb/AlN/Nb mixers with $J_c \approx 30 \, kA \, cm^{-2}$ (heavy) and $J_c \approx 10 \, kA \, cm^{-2}$ (light) current densities. The measured receiver responses are indicated by histograms, and the model fits to these are the dashed curves. For the high-current-density mixer, we infer $\omega RC = 1$ at 270 GHz, whereas for the low current density mixer, $\omega RC = 1$ at 110 GHz.
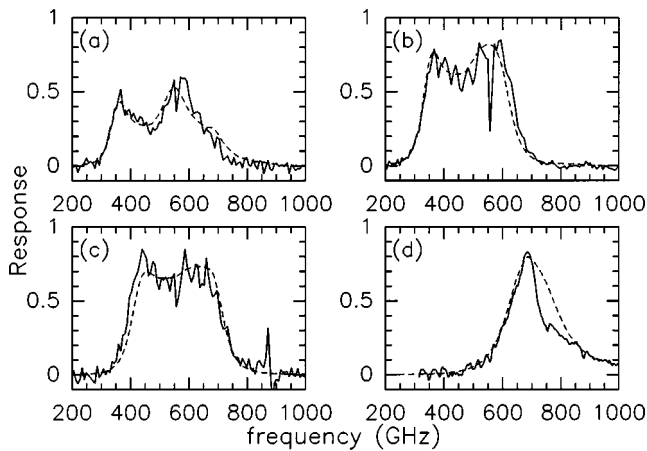
FIG. 3. Direct detection FTS response plotted with mixer model calculations for a number of different mixers with very high-current-density junctions: (a) a 550 GHz mixer with junction area $A = 0.8 \ \mu m^2$; (b) 550 GHz mixer, $A = 1.3 \ \mu m^2$; (c) 650 GHz mixer, $A = 1.7 \ \mu m^2$; and (d) 750 GHz mixer, $A = 1.0 \ \mu m^2$.

ments. In our simulations, the normal-state resistivity $\rho_n$ is only used as a scaling parameter for the Mattis–Bardeen complex conductivity, so adjusting $\rho_n$ is equivalent to changing the penetration depth. The FTS curves are quite well described by the model, and provide tight constraints on the physical parameters. The junction specific capacitance $C_s$ can be calculated by dividing the junction capacitance used in the mixer model by the junction area. The junction areas are inferred from the junction resistance $R_N$, by assuming that the resistance-area product $R_N A$ is constant across the wafer and is given by the value deduced from a set of test junctions with a wide range of junction areas.

From the mixer models, we find $\rho = 4 \ \mu \Omega$ cm for the Nb film normal-state resistivity and $C_s = 105$ fF $\mu m^{-2}$ for the specific capacitance of the high-current-density junctions. The specific capacitance for the low-$J_c$ AlN junctions is found to be $C_s = 85$ fF $\mu m^{-2}$, which is very similar to that of AlOx barrier junctions with the same current density. The value for the normal-state resistivity is consistent with that actually measured for similar films. By combining the junction capacitance determined by modeling with the junction resistance (trivially determined from dc measurements), we find that $\omega R_N C = 1$ at 270 GHz for the high-current-density mixers. For comparison, for the low-current-density mixers, we find $\omega R_N C = 1$ at 110 GHz, which is close to that attained with Nb/AlOx/Nb junctions. Thus, the $R_N C$ product of the high-current-density junction mixers represents an improvement by a factor $\sim 2.5$ over what is presently attainable from Nb/AlOx/Nb junctions. Note that our determination of the $R_N C$ product does not depend on accurate knowledge of the junction area; the area is needed only to calculate the specific capacitance.

Finally, the sensitivity of a high-current-density mixer was measured using the standard $Y$-factor technique. For a mixer designed for operation near 550 GHz, we measured a double-sideband receiver noise temperature of $T_{RX} = 110$ K at 530 GHz, with no corrections applied. The spectral response of this mixer is shown in Fig. 3(b), and its current–voltage characteristics and intermediate frequency (if) output power in response to hot (295 K) and cold (77 K) loads are shown in Fig. 1. We stress that the mixer circuit design was optimized for a junction with $R_N A \approx 20 \ \Omega \ \mu m^2$, so the coupling is not optimal at either the if or the rf. Regardless, the performance at 530 GHz is still excellent and is comparable to our best results with this mixer design and receiver configuration when employing lower-$J_c$ Nb/AlOx/Nb mixers. This measurement confirms that the high-current-density junctions used in our study are capable of low-noise mixing.

The use of high-current-density SIS mixers should greatly advance the development of low-noise terahertz mixers. Generally, it should greatly relax the requirements on the losses in tuning circuits. In particular, it should be possible to improve the noise performance of a mixer that uses a normal-metal tuning circuit by a factor of at least 2 near 1 THz. Finally, the reduction in the $R_N C$ product naturally allows the construction of mixers with very large input bandwidths. This is important especially at higher frequencies where the wider bandwidth allows a given frequency range to be covered with fewer mixers, resulting in simplified instrument designs.

[1] J. Carlstrom and J. Zmuidzinas, in *Review of Radio Science 1993–1996*, edited by W. R. Stone (Oxford University Press, Oxford, 1996), pp. 839–882.

[2] J. R. Tucker, IEEE J. Quantum Electron. **15**, 1234 (1979).

[3] J. R. Tucker and M. J. Feldman, Rev. Mod. Phys. **57**, 1055 (1985).

[4] M. Bin, M. C. Gaidis, J. Zmuidzinas, T. G. Phillips, and H. G. LeDuc, Appl. Phys. Lett. **68**, 1714 (1996).

[5] J. Kawamura, J. Chen, D. Miller, J. Kooi, J. Zmuidzinas, B. Bumble, H. G. LeDuc, and J. A. Stern, Appl. Phys. Lett. **75**, 4013 (1999).

[6] R. E. Miller, W. H. Mallison, A. W. Kleinsasser, K. A. Delin, and E. M. Macedo, Appl. Phys. Lett. **63**, 1423 (1993).

[7] A. W. Kleinsasser, R. E. Miller, W. H. Mallison, and G. B. Arnold, Phys. Rev. Lett. **72**, 1738 (1994).

[8] A. W. Kleinsasser, W. H. Mallison, and R. E. Miller, IEEE Trans. Appl. Supercond. **5**, 2318 (1995).

[9] M. C. Gaidis, H. G. LeDuc, M. Bin, D. Miller, J. A. Stern, and J. Zmuidzinas, IEEE Trans. Microwave Theory Tech. **44**, 1130 (1996).

[10] B. Bumble, H. G. LeDuc, and J. A. Stern, in *Proceedings of the 9th International Symposium on Space THz Technology*, edited by W. R. McGrath (Jet Propulsion Laboratory, Pasadena, CA, 1998), pp. 295–304.

[11] J. Zmuidzinas, H. G. LeDuc, J. A. Stern, and S. R. Cypher, IEEE Trans. Microwave Theory Tech. **42**, 698 (1994).

[12] D. C. Mattis and J. Bardeen, Phys. Rev. **111**, 412 (1958).